Broadband Noise Generation by a Vortex Model of Cavity Flow

Jay C. Hardin* and Jean P. Mason†
NASA-Langley Research Center, Hampton, Va.

This paper presents a potential flow model of two-dimensional cavity flow in which the shear layer is represented by discrete rectilinear vortices. The model compares favorably with physical features of real cavity flows. A theory is developed through which the noise generation by the cavity may be evaluated. Calculations of the spectra and directivity of the quadrupole noise source determined by this theory explain frequency and directivity phenomena observed in airframe noise testing of real aircraft.

Introduction

THE importance of airframe noise as the floor under further propulsive noise reduction and as a design consideration in future aircraft has been stressed by many researchers, including Morgan and Hardin.[1] Recent data[2] indicate that one of the most intense sources of such radiation on landing approach is produced by the wheel cavities of the aircraft in that a significant broadband increase in the noise spectrum is observed when the wheel wells are opened and the landing gear deployed. Although it is not yet clear whether this noise increase is due to the cavity itself or to a change in the flowfield around the wing/flap system, considerable research into the noise generation mechanisms of cavity flow has been stimulated.

The flowfield within cavities has been of interest for several years due to fatigue and buffeting problems. Extensive data on cavity flowfields have been obtained and methods for the reduction of internal pressure oscillations have been developed.[3] However, little is now known of the farfield radiation of cavities with the exception of the tonal behavior which can occur in certain ranges of Mach number and cavity dimensions.[4] Although tones have been observed in the airframe-noise signature of some aircraft, it is apparent that this is not the only mechanism present at the low approach Mach numbers of modern airliners.

In an attempt to attain an understanding of such mechanisms and develop methods for their reduction, this paper presents a model of two-dimensional cavity flow in which a shear layer over the cavity is represented by discrete rectilinear vortices which are free to move as the flow progresses. Such models have proven useful in the understanding of flowfields—a rather thorough review is given by Clements and Maull[5]—and have been employed in the calculation of noise production in jets by Davies et al.[6] Although the model is initially started impulsively, the computation is continued until a statistically steady flow is achieved. The noise production by the cavity is then evaluated through a reformulation of Lighthill's theory employing an extension of the "reflection principle."[7] The paper presents results on the spectrum and directivity of cavity broadband noise generation calculated on the basis of this theory.

Approach

A visualization of the flow over and within a cavity is shown in Fig. 1. This photograph was obtained by H. Werle of ONERA in a low-speed water tunnel. The length-to-depth ratio of the cavity is 2.0, the flow speed is 10 cm/sec, and the flow direction is from left to right. It can be seen that the flow separates at the leading edge of the cavity creating a highly vortical shear layer between the fluid within the cavity and the flow outside. This shear layer spreads into the cavity, ultimately impinging on the back wall, and turns downward creating a large relatively stable vortex trapped within the cavity. This vortex, which is fed energy by the shear layer, interacts with it inducing a semiperiodic displacement of the shear layer which governs the rate at which vorticity is shed downstream.

In this analysis, a model of this flow is developed through the use of simple potential solutions. The model is based upon a Schwarz-Christoffel relation which transforms the cavity geometry into a plane. The inviscid cavity flow is obtained from the complex potential of uniform flow over a plane. Separation of this flow at the cavity leading edge is then simulated by the insertion of discrete vortices near the leading edge. One vortex is inserted during each small time interval Δt. The circulation of these discrete vortices is determined by application of the Kutta condition at the leading edge. Their position in the transform plane is obtained by numerical inversion of the transformation and the boundary condition of zero normal velocity at the walls satisfied by the insertion of image vortices. The motion of the shear layer can then be followed by sequential solution of the governing potential flow equations in time.

Inviscid Flowfield of a Cavity

Consider a general two-dimensional cavity of length L and depth D as shown in Fig. 2 where it is assumed that far up and downstream of the cavity the flow is uniform and parallel to the x' axis. Employing the nondimensional variables

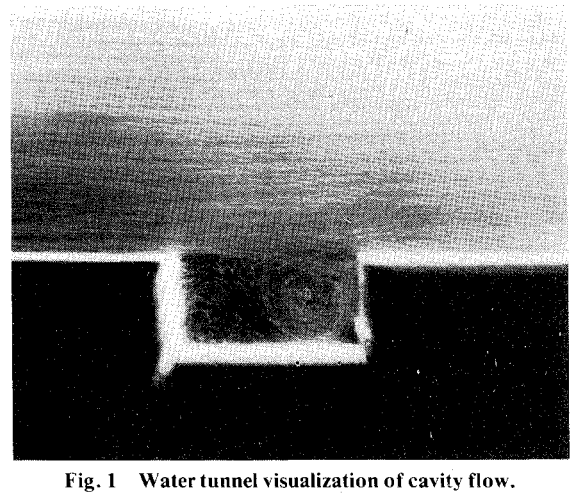

Fig. 1 Water tunnel visualization of cavity flow.

Presented at the 3rd AIAA Aero-Acoustics Conference, Palo Alto, Calif., July 20-22, 1976; submitted July 20, 1977; revision received Jan. 27, 1976.

Index categories: Aircraft Noise, Aerodynamics; Jets, Wakes, and Viscid-Inviscid Flow Interactions.

*Head, Theoretical Acoustics Group.

†Mathematician.

$$x=\frac{2x'}{L} \quad y=\frac{2y'}{L} \tag{1}$$

yields the geometry shown in Fig. 3(a) where $d=2D/L$. The normalized flow velocity then becomes $U_0=2U_0'/L$. If the complex variable $z=x+iy$ is introduced, R.R. Clements[8] of the University of Bristol has shown that the cavity and wall may be transformed into the real axis of the λ-plane shown in Fig. 3(b) by the transformation

$$z=\frac{E[\sin^{-1}\lambda \setminus \sin^{-1}(1/a)]}{E(1/a^2)} \tag{2}$$

where $\lambda=\zeta+i\eta$, $E[\cdot \setminus \cdot]$ is the incomplete elliptical integral of the second kind with complex argument and $E(\cdot)$ is the complete elliptical integral of the second kind.[9] This transformation takes the points $z=\pm 1$ into the points $\lambda \pm 1$ and the points $z=\pm 1+id$ into the points $\lambda=\pm a$. Thus, the parameter a must satisfy the relation

$$1+id=\frac{E[\sin^{-1}a \setminus \sin^{-1}(1/a)]}{E(1/a^2)} \tag{3}$$

However, it can be shown[10] that

$$E[\sin^{-1}a \setminus \sin^{-1}(1/a)]=E(1/a^2)+i[K(1-1/a^2) - E(1-1/a^2)]$$

where $K(\cdot)$ is the complete elliptical integral of the first kind. Thus,

$$d=\frac{K(1-1/a^2)-E(1-1/a^2)}{E(1/a^2)} \tag{4}$$

The solution of this relation for the parameter a is shown in Fig. 4.

The uniform velocity far up and downstream of the cavity may be introduced by recalling that the complex potential is invariant under a conformal transformation such as that given by Eq. (2). In the transform λ-plane, the flow will appear as a uniform flow in the ζ direction with the simple potential

$$w(\lambda)=A\lambda$$

where A is a constant. Thus, in the original z-plane

$$w(z)=Af(z) \tag{5}$$

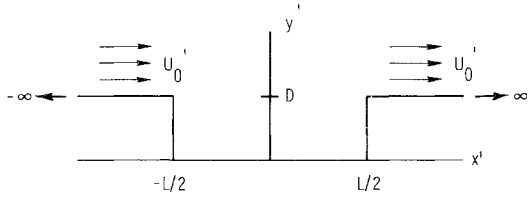

Fig. 2 Cavity geometry.

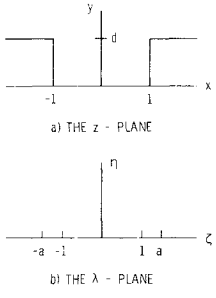

Fig. 3 The coordinate transformation.

where $\lambda=f(z)$ is the inversion of the transformation. The irrotational velocity components in the z-plane may then be calculated from

$$u-iv=\frac{dw}{dz}=\frac{dw}{d\lambda}\frac{d\lambda}{dz}=Af'(z) \tag{6}$$

where

$$f'(z)=\frac{d\lambda}{dz}=aE(1/a^2)\frac{(\lambda^2-1)^{1/2}}{(\lambda^2-a^2)^{1/2}}$$

by Eq. (2). Applying the known condition that $u \to U_0$ as $|z| \to \infty$ yields $A=U_0/aE(1/a^2)$.

Effect of Viscosity on the Cavity Flow

Although the solution obtained in the previous section is perfectly valid as long as the flow is inviscid, real flows are viscous. The action of viscosity on the flow is to introduce an additional force which places restrictions on the flow's behavior. In particular, as the flow reaches the leading edge of the cavity, it will no longer turn the corner as it does in the potential flow case but will, instead, separate from the surface creating a shear layer between the outer flow and the more quiescent fluid within the cavity.

This shear layer is made up of highly rotational fluid as a result of the creation of vorticity by the surface and is highly unstable, tending to roll up due to the Kelvin-Helmholtz instability into concentrated regions of high vorticity. Thus, the potential flow solution can be modified to include this shear layer by the periodic insertion of two-dimensional vortex filaments near the leading edge of the cavity. Such a model has been successfully employed in the case of a square-based section by Clements.[11]

Suppose that, at time t, there are N vortices of strengths Γ_i at the positions z_i $(i=1,2,\ldots N)$. Then, the velocity at any point in the flow will consist of the irrotational flow given by Eq. (6) in addition to the velocity induced by the vortices. If $\lambda_i=f(z_i)$ are the transforms of the vortex positions, the complex potential is given by

$$w(\lambda)=A\lambda-\frac{i}{2\pi}\sum_{i=1}^{N}\Gamma_i\log(\lambda-\lambda_i) + \frac{i}{2\pi}\sum_{i=1}^{N}\Gamma_i\log(\lambda-\lambda_i^*) \tag{7}$$

where the star indicates the complex conjugate and the second summation consists of the image vortices necessary to satisfy the boundary condition of no flow through the plane $\eta=0$. Thus, the velocities are given by

$$u-iv=dw/dz=\left[A-\frac{i}{2\pi}\sum_{j=1}^{N}\frac{\Gamma_j}{(\lambda-\lambda_j^*)} + \frac{i}{2\pi}\sum_{j=1}^{N}\frac{\Gamma_j}{(\lambda-\lambda_j^*)}\right]f'(z) \tag{8}$$

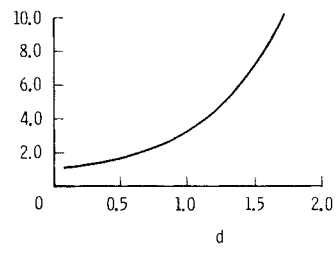

Fig. 4 the parameter a as a function of non-dimensional depth.

If the point at which the velocity is desired is a point where a vortex occurs, say $z=z_k$, then Rough's rule[11]

$$(u-iv)\Big|_{z=z_k}=\left[A-\frac{i}{2\pi}\sum_{\substack{j=1\\ j\neq k}}^{N}\frac{\Gamma_j}{(\lambda_k-\lambda_j)}+\frac{i}{2\pi}\sum_{j=1}^{N}\frac{\Gamma_j}{(\lambda_k-\lambda_j^*)}\right]f'(z_k)-i\frac{\Gamma_k}{4}\frac{f''(z_k)}{f'(z_k)} \tag{9}$$

where $\lambda_k=f(z_k)$.

The rate at which vorticity is shed into the shear layer, and thus the circulation Γ_i of these vortices, is thought to be governed by the relation $d\Gamma/dt=U_s^2/2$, where U_s is the velocity at the outer edge of the boundary layer as suggested by Clements.[11] However, the boundary-layer thickness is unknown, and application of this condition with $U_s=U_0$ led to a model which was not physically realistic. The vorticity was nearly all trapped in the cavity forming a single large vortex which ultimately rose out into the flow. A more physically realistic model can be obtained by application of the Kutta condition at the leading edge of the cavity. This condition requires that the transform of the leading edge ($\lambda=-a$) be a stagnation point in the transform plane. Suppose that, at time t, there are $N-1$ vortices in the flow and that a new vortex is introduced at the point z_N. If $\lambda_N=f(z_N)$, then the point $\lambda=-a$ will be a stagnation point in the transform plane if the circulation of the new vortex is taken as

$$\Gamma_N=\frac{-\pi A-\sum_{i=1}^{N-1}\dfrac{\Gamma_i I_m\lambda_i}{a^2+2aRe\lambda_i+|\lambda_i|^2}}{\dfrac{I_m\lambda_N}{a^2+2aRe\lambda_N+|\lambda_N|^2}} \tag{10}$$

where $Re(\cdot)$ and $I_m(\cdot)$ indicate the real and imaginary parts of a complex number.

Operation of the Cavity Model

The model for two-dimensional cavity flow developed in the previous two sections may be readily exercised by numerical integration of the governing equations in time. The flow is started from rest. There seem to be two equally valid ways of viewing this starting process depending upon the preference of the individual. It can be assumed that the time-independent potential flow over the cavity exists and that, at time $t=0$, viscosity is "turned on" and vorticity begins to be shed into the shear layer. Or the concept of an "impulsive start" may be envisioned. This requires that at $t=0$, the potential flow be established essentially instantaneously and then subsequently modified by the action of viscosity.

Whichever of these starting processes is pictured, in the first small time interval Δt, a short length of vortex sheet will be shed from the cavity leading edge into the shear layer. This short length of sheet will tend to roll up due to the action of the Kelvin-Helmholtz instability and can thus be replaced in the model by a discrete rectilinear vortex at the position $z_1=-1+[(U_0\Delta t)/3]+ih$ which is roughly the centroid of the vortex sheet.[6] The position of this vortex in the transform plane can then be determined through numerical inversion of the transform, for example, $\lambda_1=f(z_1)$, and its circulation from Eq. (10). The velocity field experienced by this vortex in the physical plane is then given by Eq. (9) and its position at the end of the second time interval Δt obtained through numerical integration of the governing equations

$$dx/dt=u(x,y)$$

$$dy/dt=v(x,y) \tag{11}$$

However, during this second time interval Δt, another short length of vortex sheet will have been shed from the cavity leading edge. It is replaced by a new discrete vortex at the point $z=z_1$ and the process repeated. The positions of both vortices in the transform plane are obtained by inverting the transformation, the circulation of the new vortex calculated from Eq. (10), the velocity of each vortex determined from Eq. (9), and new positions through integration of Eq. (11).

This procedure can be continued for as long as desired. For dimensionless time steps $U_0\Delta t$ such that $0.01\leq U_0\,\Delta t\leq 0.1$, the macroscopic character of the flow has been shown independent of the time step by comparing models with different time steps at the same nondimensional time. The steady-state behavior is reached about $U_0t=20.0$. Motion picture films of the vortices within this flow model have been produced out to $U_0t=100.0$. For the values $1\leq l/D\leq 2$ used in this study, these films show that the shear layer rolls up into a relatively stable, large vortex within the cavity with vorticity continuously being shed downstream. A semiperiodic "sloshing" motion of the cavity flow can also be observed. Figure 5 is a blown-up frame from such a film with $U_0\,\Delta t=0.1$ and $L/D=2.0$. The dots shown are crosssections of rectilinear vortices with axes into the plane of the paper. This figure can be compared with the flow visualization of the similar cavity shown in Fig. 1. Clearly, such comparisons are tenuous as the model is basically inviscid, which makes it difficult to determine what range of Reynolds number of real flows, if any, the model simulates. However, the comparison does indicate that many physical features of the actual flow are present in the model.

There are two computational problems which arise in attempts to utilize this model. The first is the required inversion of the transformation. For a given vortex position z, a Newton-Raphson iteration procedure is used to find the value of λ which satisfies Eq. (2). Since λ is a complex variable, this requires that the elliptic integral $E[\sin^{-1}\lambda\setminus\sin^{-1}(1/a)]$ be transformed into an expression containing elliptic integrals with only real arguments. These integrals are then evaluated by the process of arithmetic-geometric mean.[9] This procedure works well unless the vortices are very close to the walls of the cavity, which is the second of the computational problems which arise. This problem has been overcome by removing from the calculation any vortices which approach closer than 0.015 to the walls, a solution first suggested by Clements,[11] who implied that it was physically equivalent to viscous dissipation of vorticity.

Theory of Cavity Noise Radiation

Since this study is motivated by sound generation due to the presence of the cavity, it is necessary to consider how such radiation might be related to the parameters of the model.

Fig. 5 The cavity model.

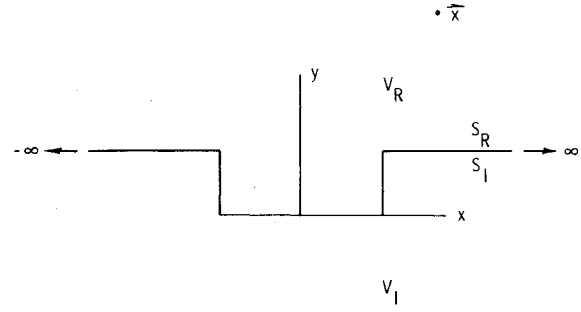

Fig. 6 Real and image spaces.

Certainly, the model itself is incompressible. Thus, such a theory must ultimately rest upon the work of Crow,[12] who has shown that the relevant sound sources may be considered to be the incompressible (and, in fact, solenoidal!) components of velocity within the turbulent flowfield. With this result in mind, a simple expression for the noise radiation by the cavity may be obtained by a slight extension of the "reflection principle" ideas first set forth by Powell.[7] Consider the cavity geometry shown in Fig. 6. Curle[13] has shown that, for the case of zero normal velocity at the solid boundary, the acoustic density at the observer position x is given by

$$\rho_a(x,t) = \frac{1}{4\pi a_0^2}\frac{\partial^2}{\partial x_i \partial x_j}\int_{V_R}\frac{T_{ij}^{(R)}(y,t-r/a_0)}{r}\,dy - \frac{1}{4\pi a_0^2}\frac{\partial}{\partial x_i}\int_{S_R}\frac{P_i^{(R)}(y,t-r/a_0)}{r}\,dy \tag{12}$$

where $T_{ij}^{(R)}$ is Lighthill's stress tensor in the region V_R and $P_i^{(R)}$ is the force per unit area exerted on the fluid by the solid boundary S_R in the i direction. The ambient speed of sound is denoted by a_0 and $r = |x-y|$. Lighthill's stress tensor and the surface pressures can be related to the real vortices in the volume V_R.

The image vortices within the volume V_I may also be considered to generate a Lighthill stress tensor $T_{ij}^{(I)}$ and pressures $P_i^{(I)}$ on the surface S_I. Thus, an equation similar to Eq. (12) may be written for the image space. However, since the observer position x is separated from the region V_I by the solid surface S_I, there can be no radiation to x from the image space (see Ffowcs-Williams)[14] and the expression must be identically zero, that is,

$$0 = \frac{1}{4\pi a_0^2}\frac{\partial^2}{\partial x_i \partial x_j}\int_{V_I}\frac{T_{ij}^{(I)}(y,t-r/a_0)}{r}\,dy - \frac{1}{4\pi a_0^2}\frac{\partial}{\partial x_i}\int_{S_I}\frac{P_i^{(I)}(y,t-r/a_0)}{r}\,dy \tag{13}$$

Thus, adding Eqs. (12) and (13) yields

$$\rho_a(x,t) = \frac{1}{4\pi a_0^2}\frac{\partial^2}{\partial x_i \partial x_j}\int_{V_R+V_I}\frac{T_{ij}(y,t-r/a_0)}{r}\,dy - \frac{1}{4\pi a_0^2}\frac{\partial}{\partial x_i}\int_{S_R}\frac{P_i^{(R)}(y,t-r/a_0)}{r}\,dy - \frac{1}{4\pi a_0^2}\frac{\partial}{\partial x_i}\int_{S_I}\frac{P_i^{(I)}(y,t-r/a_0)}{r}\,dy \tag{14}$$

where T_{ij} takes the value $T_{ij}^{(R)}$ or $T_{ij}^{(I)}$ depending upon the region where the point y lines.

Now, Powell[7] has shown that the sum of the two surface integrals in Eq. (14) is zero for inviscid flow over an infinite plane surface. However, this is not necessarily true for the cavity geometry as the image flow is no longer a mirror reflection of the real flow. For this case, noting that the model is inviscid, Eq. (14) can be written

$$\rho_a(x,t) = \frac{1}{4\pi a_0^2}\frac{\partial^2}{\partial x_i \partial x_j}\int_{V}\frac{T_{ij}(y,t-r/a_0)}{r}\,dy + \frac{1}{4\pi a_0^2}\frac{\partial}{\partial x_n}\int_{S_R}\frac{\Delta P(y,t-r/a_0)}{r}\,dy \tag{15}$$

where ΔP is the surface pressure discontinuity across the boundary surface produced by the difference in the real and image flows and n is the outward normal to the surface S_R. This relation, which could have been obtained directly from Eqs. (3.1) and (3.2) of Ffowcs-Williams' paper,[14] shows that the sound radiation can be expressed as a distribution of quadrupoles over both the real and image spaces as if the surface were not present and a residual distribution of dipoles over the surface whose strength depends upon the pressure differential caused by the imperfect reflection due to the cavity in the surface.

The major advantage of Eq. (15) over Eq. (12) is that the description of mere reflection of the quadrupole sound by the surface has been removed from the surface integral into the volume integral where it may be more easily calculated. To see this, note that in the absence of surfaces,

$$\frac{1}{4\pi a_0^2}\frac{\partial^2}{\partial x_i \partial x_j}\int_{V}\frac{T_{ij}(y,t-r/a_0)}{r}\,dy = \frac{1}{4\pi a_0^2}\int_{V}\frac{\delta^2}{\delta y_i \delta y_j}\frac{T_{ij}(y,t-r/a_0)}{r}\,dy \tag{16}$$

where $\delta/\delta y_i$ indicates partial differentiation with respect to y_i with r held fixed. This latter integral has been studied by Hardin[15] who has shown that, in the far field

$$\frac{1}{4\pi a_0^2}\int_{V}\frac{\delta}{\delta y_j}\frac{T_{ij}(y,t-r/a_0)}{r}\,dy \simeq -\frac{\rho_0}{4\pi a_0^4}\frac{x_i x_j}{x^3}\left(\frac{d^2}{dt^2}\int_{V} y_i \mathfrak{L}_j\,dy\right)^* + \frac{1}{4\pi a_0^4}\frac{1}{x}\left(\frac{d^2 e}{dt^2}\right)^* \tag{17}$$

Here $\mathfrak{L} = \Omega \times v$, where Ω is the vorticity and v the solenoidal velocity; the asterisk indicates evaluation at the retarded time $t - x/a_0$ and

$$e = \rho_0\int_{V}\frac{v^2}{2}\,dy \tag{18}$$

is the total kinetic energy of the solenoidal field. Thus, taking a similar farfield approximation for the surface integral, Eq. (15) becomes

$$\rho_a(x,t) \simeq -\frac{\rho_0}{4\pi a_0^4}\frac{x_i x_j}{x^3}\left(\frac{d^2}{dt^2}\int_{V} y_i \mathfrak{L}_j\,dy\right)^* + \frac{1}{4\pi a_0^4}\frac{1}{x}\left(\frac{d^2 e}{dt^2}\right)^* + \frac{1}{4\pi a_0^3}\frac{x_i}{x^2}\left(\frac{d}{dt}\int_{S_R}\Delta P\,dy\right)^* \tag{19}$$

which is a theoretical expression for noise radiation by a cavity.

Quadrupole Noise Radiation by the Model

Note that Eq. (19) implies that there are actually three potential types of sources associated with a cavity in a flowfield. The lowest order is a monopole produced by the second-time derivative of the solenoidal kinetic energy. As the Kutta condition results in a nonconstant rate of introduction of vorticity, this term should be important and, in fact, may account for the intense tones which can be produced by cavities in certain ranges of Mach number and L/D. The next higher-order source is a distribution of dipoles over the surface related to the discontinuity of pressure across it. Powell[7] has shown that this term is identically zero in the absence of the cavity. Thus, its contribution is probably

small, at least for shallow cavities. The highest-order term is a distribution of quadrupoles over the entire (real and imaginary) volume occupied by the flow and is undoubtedly primarily responsible for broadband noise generation by the cavity. It is this term which has been pursued in calculation of broadband noise production by the model.

Consider the integral

$$\int_V y_i \mathfrak{L}_j \mathrm{d}V$$

for a field of rectilinear vortices. Suppose that, at time t, there are N real vortices in the field with circulations $\Gamma(n) = 1,2,\ldots,N$. There are also N imaginary vortices within circulations $\Gamma(n) = -1,-2,\ldots,-N$. Then, since vorticity only occurs within the cores of the vortices,

$$\int_V y_i \mathfrak{L}_j \mathrm{d}V = \sum_{n=N}^{N} \int_V y_1 \mathfrak{L}_j{}^{(n)} \mathrm{d}y \tag{20}$$

where the convention $\mathfrak{L}_j{}^{(0)} = 0$ has been adopted.

Now, in the standard Cartesian coordinate space, if it is assumed that vorticity is uniformly distributed over the core of each vortex

$$\Omega^{(n)} = \frac{\Gamma^{(n)}}{A} k \tag{21}$$

where A is the area of the core. Further

$$v = u^{(n)} i + v^{(n)} j \tag{22}$$

where $u^{(n)}$ and $v^{(n)}$ are the x and y components of velocity induced on the core of the nth vortex by all the other vortices. Thus

$$\mathfrak{L}^{(n)} = \Omega^{(n)} \times v^{(n)} = -\frac{v^{(n)}\Gamma^{(n)}}{A} i + \frac{u^{(n)}\Gamma^{(n)}}{A} j \tag{23}$$

and it can be seen that $\mathfrak{L}_3{}^{(n)} = 0$. Therefore

$$\int_V y_i \mathfrak{L}_3{}^{(n)} \mathrm{d}y = 0 \tag{24}$$

Further, since $\mathfrak{L}^{(n)}$ is independent of z

$$\int_V y_3 \mathfrak{L}_j{}^{(n)} \mathrm{d}y = 0 \tag{25}$$

Thus, there are only four nonzero components of the integral

$$\int_V y_1 \mathfrak{L}_1{}^{(n)} \mathrm{d}y = -x^{(n)} v^{(n)} \Gamma^{(n)} \ell \tag{26a}$$

$$\int_V y_2 \mathfrak{L}_1{}^{(n)} \mathrm{d}y = -y^{(n)} v^{(n)} \Gamma^{(n)} \ell \tag{26b}$$

$$\int_V y_1 \mathfrak{L}_2{}^{(n)} \mathrm{d}y = x^{(n)} u^{(n)} \Gamma^{(n)} \ell \tag{26c}$$

and

$$\int_V y_2 \mathfrak{L}_2{}^{(n)} \mathrm{d}y = y^{(n)} u^{(n)} \Gamma^{(n)} \ell \tag{26d}$$

where $x^{(n)}$ and $y^{(n)}$ are the coordinates of the position of the nth vortex at the time t and ℓ is the nominal length of the vortices in the z direction.

Thus, the quadrupole term of Eq. (19) becomes

$$\rho_a(x,t) \simeq -\frac{\rho_0}{4\pi a_0^4}\left[\frac{x_1^2}{x^3}\left(\frac{\mathrm{d}^2}{\mathrm{d}t^2}\int_V y_1 \mathfrak{L}_1 \mathrm{d}y\right)^* + \frac{x_1 x_2}{x^3}\left(\frac{\mathrm{d}^2}{\mathrm{d}t^2}\int_V y_1 \mathfrak{L}_2 \mathrm{d}y\right)^* + \frac{x_2 x_1}{x^3}\left(\frac{\mathrm{d}^2}{\mathrm{d}t^2}\int_V y_2 \mathfrak{L}_1 \mathrm{d}y\right)^* + \frac{x_2^2}{x^3}\left(\frac{\mathrm{d}^2}{\mathrm{d}t^2}\int_V y_2 \mathfrak{L}_2 \mathrm{d}y\right)^*\right] \tag{27}$$

or

$$\rho_a(x, t+x/a_0) = -\frac{\rho_0 \ell}{4\pi a_0^2 x^3}\left[-x_1^2 \frac{\mathrm{d}^2}{\mathrm{d}t^2}\sum_{\substack{n=-N \\ n\neq 0}}^{N} x^{(n)} v^{(n)} \Gamma^{(n)} + x_1 x_2 \frac{\mathrm{d}^2}{\mathrm{d}t^2}\sum_{n=-N}^{N} \Gamma^{(n)}(x^{(n)} u^{(n)} - y^{(n)} v^{(n)}) + x_2^2 \frac{\mathrm{d}^2}{\mathrm{d}t^2}\sum_{\substack{n=-N \\ n\neq 0}}^{N} \Gamma^{(n)} y^{(n)} u^{(n)}\right] \tag{28}$$

Equation (28) may be employed to readily calculate the quadrupole noise generation by the model.

Results of Cavity Noise Calculation

The broadband noise generation of a cavity has been calculated on the basis of the theory presented in the previous two sections. This was accomplished by first running the model until the steady state was reached and then computing a stationary record of farfield density fluctuation through Eq. (28). Extensive care was taken to insure that the second time derivatives required by this expression were accurately calculated. The discrete time series so generated could then be analyzed by ordinary digital spectral techniques to determine the spectra and overall levels of the noise.

Figure 7 shows a typical third octave band spectrum obtained in this way for a position directly above the cavity. The spectra for other positions are quite similar. This spectral estimate contains six degrees of freedom. Note that the spectrum is quite broadband with a peak at the Strouhal number ($St = fL/U_0'$) of 4.0. This is considerably above the Strouhal range ($0.5 \leq St \leq 2.0$) where cavity tones are normally produced. Thus, it helps to explain the high-frequency

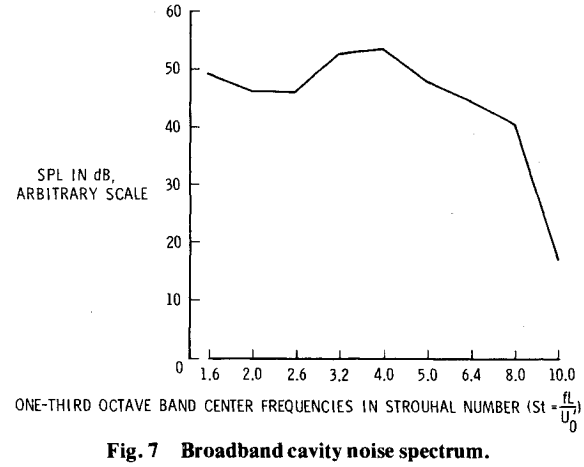

Fig. 7 Broadband cavity noise spectrum.

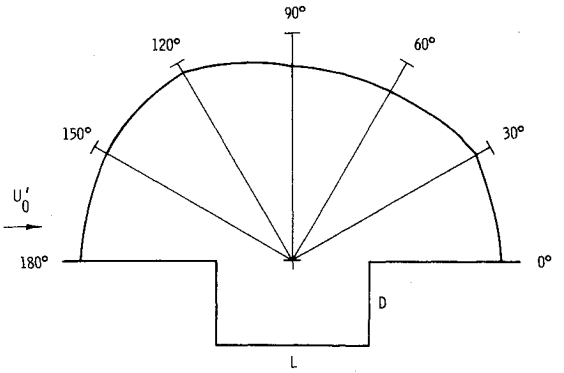

Fig. 8 Directivity of cavity broadband noise.

broadband noise generation by cavities observed during airframe noise testing of real aircraft. Figure 8 displays the calculated directivity pattern of this broadband noise source. Note that the noise peaks slightly upstream of the cavity. This effect has also been observed in full-scale airframe noise tests.

Conclusion

This paper has presented a potential flow model of two-dimensional cavity flow in which the shear layer is represented by discrete rectilinear vortices. The model compares favorably with physical features of real cavity flows. A theory is also developed through which the noise generation by the cavity may be evaluated. Calculations of the spectra and directivity of the quadrupole noise source determined by this theory explain frequency and directivity phenomena observed in airframe noise testing of real aircraft.

References

[1]Morgan, H.G. and Hardin, J.C., "Airframe Noise —The Next Aircraft Noise Barrier," *Journal of Aircraft,* Vol. 12, July 1975, pp. 622–624.

[2]Hardin, J.C., Fratello, D.J., Hayden, R.E., Kadman, Y., and Africk, J., "Prediction of Airframe Noise," NASA, TN D-7821.

[3]Heller, H.H. and Bliss, D.B., "The Physical Mechanism of Flow-Induced Pressure Fluctuations in Cavities and Concepts for Their Suppression," AIAA Paper 75-491, Hampton, Va., March 1975.

[4]Block, P.J. and Heller, H., "Measurements of Farfield Sound Generation From a Flow Excited Cavity," NASA TM X-3292, Dec. 1975.

[5]Clements, R.R.and Maull, D.J., "The Representation of Sheets of Vorticity by Discrete Vortices," *Progress in Aerospace Sciences,* Vol. 16, 1975, pp. 129–146.

[6]Davies, P.O.A.L., Hardin, J.C., Edwards, A.V.J., and Mason, J.P., "A Potential Flow Model for Calculation of Jet Noise," AIAA Paper 75-441, Hampton, Va., March 1975.

[7]Powell, A., "Aerodynamic Noise and the Plane Boundary," *JASA,* Vol. 32, Aug. 1960, pp. 982–990.

[8]Clements, R.R., Private communication, 1975.

[9]Abramowitz, M. and Stegun, I.A., "Handbook of Mathematical Functions," National Bureau of Standards, p. 598, June 1964.

[10]Byrd, P.F. and Friedman, M.D., *"Handbook of Elliptical Integrals for Engineers and Physicists,"* Springer-Verlag, 1954, p. 11.

[11]Clements, R.R., "An Inviscid Model of Two-Dimensional Vortex Shedding," *Journal of Fluid Mechanics,* Vol. 57, 1973, pp. 321–336.

[12]Crow, S.C., "Aerodynamic Sound Emission as a Singular Perturbation Problem," *Studies in Applied Mathematics,* Vol. XLIX, March 1970, pp. 21-44.

[13]Curle, N., "The Influence of Solid Boundaries Upon Aerodynamic Sound," *Proceedings of the Royal Society,* Series A., Vol. 231, 1955, pp. 505–514.

[14]Ffowcs-Williams, J.E., "Sound Radiation From Turbulent Boundary Layers Formed on Compliant Surfaces," *Journal of Fluid Mechanics,* Vol. 22, 1965, pp. 347–358.

[15]Hardin, J.C., "Analysis of Noise Produced by an Orderly Structure of Turbulent Jets," NASA TN D-7242, April 1973.